crystals

MDPI

Article

Rheological Properties of Cement Paste Containing Ground Fly Ash Based on Particle Morphology Analysis

Juntao Ma [1,2,*], Huifang Zhang [1,2], Daguang Wang [3], Huixian Wang [1,2] and Gonglian Chen [1,2]

1 International Joint Research Lab for Eco-Building Materials and Engineering of Henan, North China University of Water Resources and Electric Power, Zhengzhou 450045, China; zhanghf317@163.com (H.Z.); whx@ncwu.edu.cn (H.W.); chengonglian@ncwu.edu.cn (G.C.)
2 Collaborative Innovation Center for Efficient Utilization of Water Resources, North China University of Water Resources and Electric Power, Zhengzhou 450045, China
3 China Construction Seventh Engineering Division Co., Ltd., Zhengzhou 450004, China; wdaguang@163.com
* Correspondence: majuntao@ncwu.edu.cn

Abstract: Separating finer particles from raw fly ash is a popular method to produce high-performance admixture of concrete. However, the supply of separated fly ash is obviously behind the demand and the residue fly ash is difficult to be disposed. Ground fly ash is another method to improve the particle size and reactivity, but the change of particle morphology during grinding may affect the rheological properties of cement paste and concrete, which limits the application of ground fly ash in concrete projects. In this study, the raw fly ash, separated fly ash, and ground fly ash of the same particle size range were studied and the particle morphology was analyzed by Image-Pro Plus process and spherical particles proportion calculation. On this basis, the fluidity and rheological properties of cement paste with different fly ash content were tested and the mechanism was discussed by packing density and zeta potential analysis. The results showed that the total amount of spherical particles in fly ash-cement paste system was reduced due to the spherical particles of ground fly ash being destroyed during the grinding process. Thus, compared with the separated fly ash of similar particle size range, the fluidity of ground fly ash was significantly decreased while the yield stress and plastic viscosity increased significantly, which indicated that the rheological properties of fly ash cement paste are closely related to the particle morphology of fly ash. The results provide theoretical basis and technology support to the application of ground fly ash.

Keywords: ground fly ash; particle morphology; rheological properties; packing density; zeta potential

Citation: Ma, J.; Zhang, H.; Wang, D.; Wang, H.; Chen, G. Rheological Properties of Cement Paste Containing Ground Fly Ash Based on Particle Morphology Analysis. *Crystals* **2022**, *12*, 524. https://doi.org/10.3390/cryst12040524

Academic Editors: José L. García and Yongli Gao

Received: 6 March 2022
Accepted: 7 April 2022
Published: 9 April 2022

1. Introduction

Fly ashes from combustion of coal, shale, or solid wastes can contain various hazardous elements [1]. Therefore, their beneficiation was subjected by several studies during last two decades [2,3]. The application of fly ash (FA) in concrete projects saves the consumption of cement in concrete and reduces carbon emissions in construction projects [4–6]. In previous studies [7–11], the morphology of most fly ash particles appeared spherical and the ball-bearing effect could improve the fluidity of concrete and enhance the construction performance of concrete. Some studies, on the other hand, showed that a high volume addition of fly ash may decrease the early strength and durability of concrete significantly, which limits the wide application of fly ash in concrete [6,12–14].

Many studies have shown that high-grade fly ash, which exhibits smaller particle size, has a lower water requirement ratio and improves the workability of fresh concrete as mineral admixture [15–19]. Furthermore, the presence of unburned carbons or chars in FAs can also have impacts on their usage as a cement admixture. Hence, the high-grade fly ash is separated from the raw fly ash in the coal-fired power plants and the output quantity is limited. Meanwhile, the residual coarser fly ash is much more difficult to be effectively applied in concrete.

In order to improve the utilization and value of fly ash, ground fly ash is one of the feasible ways to reduce the particle size and strengthen the properties. The research of Krishnaraj [20] and Zhao [21] showed that the fineness and activity of fly ash are significantly improved after grinding. Therefore, in some projects, ground fly ash is produced and used to replace the high-grade fly ash. However, a large number of studies [22–27] have also shown that some of the original spherical particles in ground fly ash are destroyed during the grinding process and turn into angular particles which decreases the ball-bearing effect and may affect the working performance of concrete. In our previous studies [28], the quantitative analysis of the spherical destruction in ground fly ash under different grinding systems was carried out. The results have shown that most of the spherical particles are destroyed after grinded in the ball mill and the fluidity of fly ash cement paste is closely related to the content of spherical particles. The rheological properties of fresh concrete containing ground fly ash is significant in the construction process while the influence law and mechanism has not been clear up until now. Most of the studies on the working performance of concrete containing ground fly ash have focused on the influence of its fluidity while the rheological properties and influence mechanism of fly ash cement paste have been seldom studied. Meanwhile, most of studies concentrated on the mechanical properties of concrete containing ground fly ash have judged the application feasibility while the workability and rheological properties have been commonly overlooked.

In this study, the particle morphology and particle size characteristics of fly ash under three different treatments were compared. The fluidity and rheological properties of cement paste were respectively analyzed according to different kinds and additions, and the mechanism was discussed combined with the packing density and zeta potential values. The relationship between the particle morphology of different fly ash and rheological properties of cement paste were analyzed, and the application feasibility of ground fly ash in high-level concrete was evaluated.

2. Materials and Methods

2.1. Materials

Fly ash used in this experiment was from Datang coal-fired power plant in Sanmenxia, China. P.O 42.5 cement was used in this experiment to prepare the cement paste. The chemical composition of fly ash and cement is listed in Table 1.

Table 1. Chemical composition of fly ash and cement (by weight, %).

Samples	SiO_2	Al_2O_3	Fe_2O_3	CaO	MgO	SO_3	Na_2O	Loss
Cement	20.63	4.45	2.88	64.06	1.67	2.88	0.54	1.55
Fly Ash	53.72	28.11	11.55	3.54	0.78	0.42	0.75	0.98

In order to study the influence of particle size and morphology on the performance, the following three different kinds of fly ash were used in this experiment:

(1) Fly ash produced directly from the power plant, denoted as raw fly ash (RFA);
(2) Fly ash separated by the pneumatic separation system which meets the requirements of fly ash of grade I in GB/T 1596-2017 "Fly Ash Used for Cement and Concrete" [29], denoted as separated fly ash (SFA); and
(3) Fly ash ground in laboratory SM-500 ball mill for 30 min, of which the particle size was equivalent to SFA, denoted as ground fly ash (GFA).

The NKT6100 laser particle size analyzer was used to test the particle size of three different fly ash particles. The specific surface area and apparent density was tested according to GB/T 8074-2008 and GB/T 208-2014, respectively. The Nova Nano450-type field emission scanning electron microscope produced by FEI Company was used to observe the particle morphology of three kinds of fly ash and the magnification was 2000×. Meanwhile, Image-Pro Plus was used to cooperate with SEM to quantify the particle morphology of fly ash.

2.2. Methods

In order to analyze the influence of fly ash particles with different particle sizes and morphology on the rheological properties of cement paste, this experiment designed different samples containing RFA, SFA, and GFA, respectively. The addition of fly ash was 0%, 10%, 20%, 30%, and 40%, and the water-binder ratio was 0.5. The cement in the experiment was P.O 42.5 cement produced by Henan Tianrui cement plant. The mix proportion of cement paste is shown in Table 2.

Table 2. Mix proportioning of cement paste containing fly ash.

Number	Addition of Fly Ash	Water/g	Cement/g	RFA/g	SFA/g	GFA/g
1	0%	250	500	0	0	0
2	10%	250	450	50	0	0
3	20%	250	400	100	0	0
4	30%	250	350	150	0	0
5	40%	250	300	200	0	0
6	10%	250	450	0	50	0
7	20%	250	400	0	100	0
8	30%	250	350	0	150	0
9	40%	250	300	0	200	0
10	10%	250	450	0	0	50
11	20%	250	400	0	0	100
12	30%	250	350	0	0	150
13	40%	250	300	0	0	200

The experiment followed the Chinese Standard GB/T8077-2012 "Methods for Testing Uniformity of Concrete Admixture" and the fluidity of cement pastes with different proportions was tested. Meanwhile, the RST-SST rheometer produced by Brookfield Company in the United States was used to test the shear stress and apparent viscosity of different fly ash, and the rheological properties were comprehensively evaluated. In the experiment, the ST-1003 type powder packing density tester was used to test the packing density of different fly ash and cement mixed systems, the DT-300 high concentration zeta potential meter was used to analyze the potential value of different fly ash in cement paste, and the mechanism of fly ash particle morphology on the rheological properties of cement paste was comprehensively analyzed.

3. Results and Discussion

3.1. Particle Morphology Analysis of Fly Ash

Particle size of three different fly ash particles is shown in Figure 1 and the particle characteristics of fly ash were calculated as shown in Table 3. The SEM morphology images are listed in Figure 2.

Table 3. Particle characteristic of different fly ash.

Fly Ash	RFA	SFA	GFA
Average particle size/μm	33.23	16.05	15.98
Specific surface area/m2·kg^{-1}	426.4	527.6	531.4
Apparent density/g·cm^{-3}	2.18	2.25	2.20

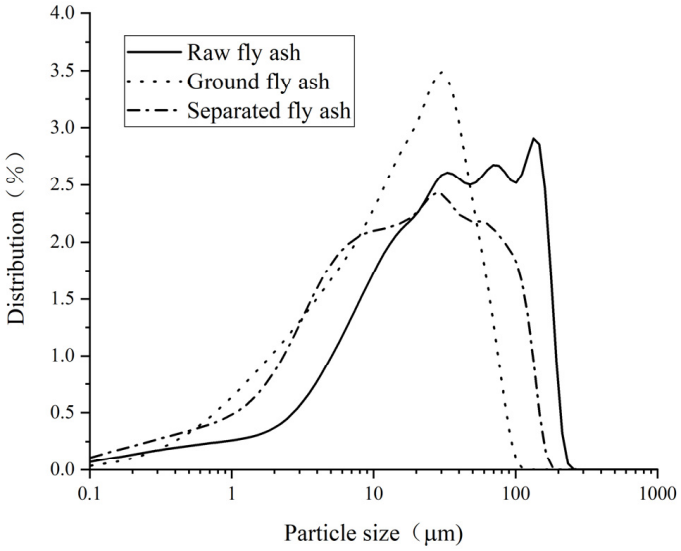

Figure 1. Particle size distribution of different fly ash.

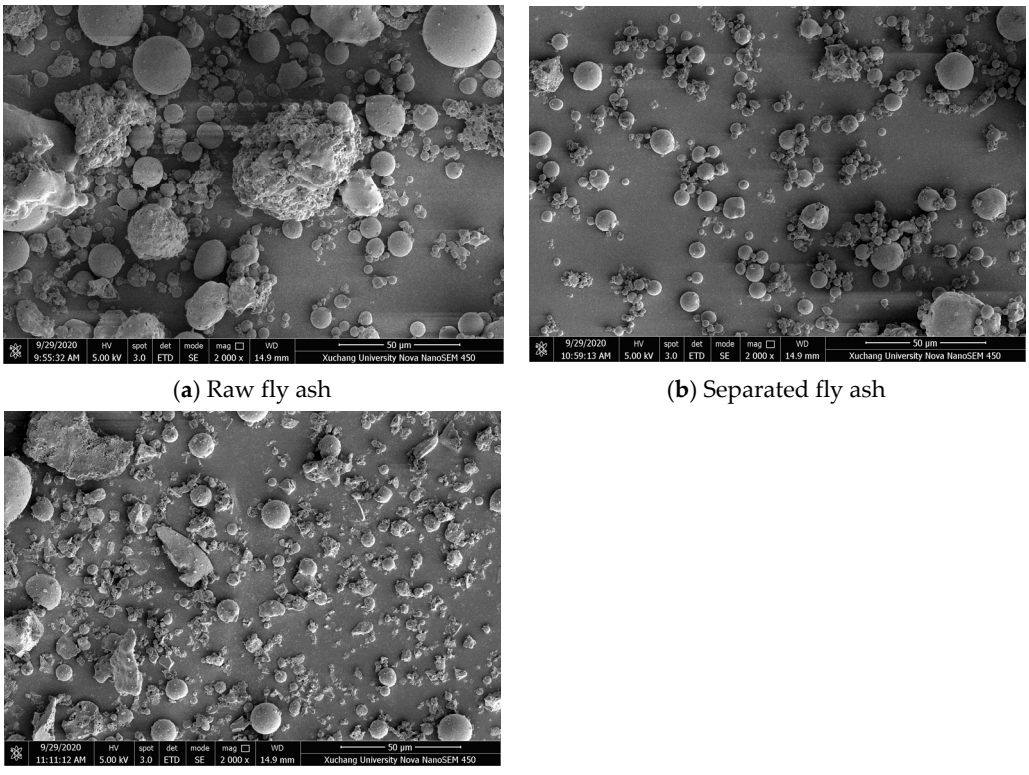

(**a**) Raw fly ash (**b**) Separated fly ash

(**c**) Ground fly ash

Figure 2. Morphology SEM-BSE images of different fly ash.

According to the particle characteristics and morphology observation of different fly ash, the particle size of RFA was the largest, of which the range was mainly between 10 μm and 250 μm. Most of the fly ash particles were spherical particles while some glass phases appeared to be irregular shapes. SFA was separated from RFA and the particle size was smaller. GFA was ground in ball mill, of which the average particle size and specific surface area was equivalent to SFA. From the observation of its microscopic morphology, the spherical particles were destroyed in long-term grinding process in the ball mill and a large number of angular particles appeared.

In order to quantify the proportion of spherical particles in different samples, Image-Pro Plus was used to calculate the area of different shape particles in the SEM-BSE images [28]. For each analyzed FA types, five random areas were chosen in the representative sample and 10 microscopic images were taken in every area. The spherical particles in 50 images were selected and painted by a different color (Figure 3) while the non-spherical particles area and interspace area were also calculated by different gray scales in Image-Pro Plus.

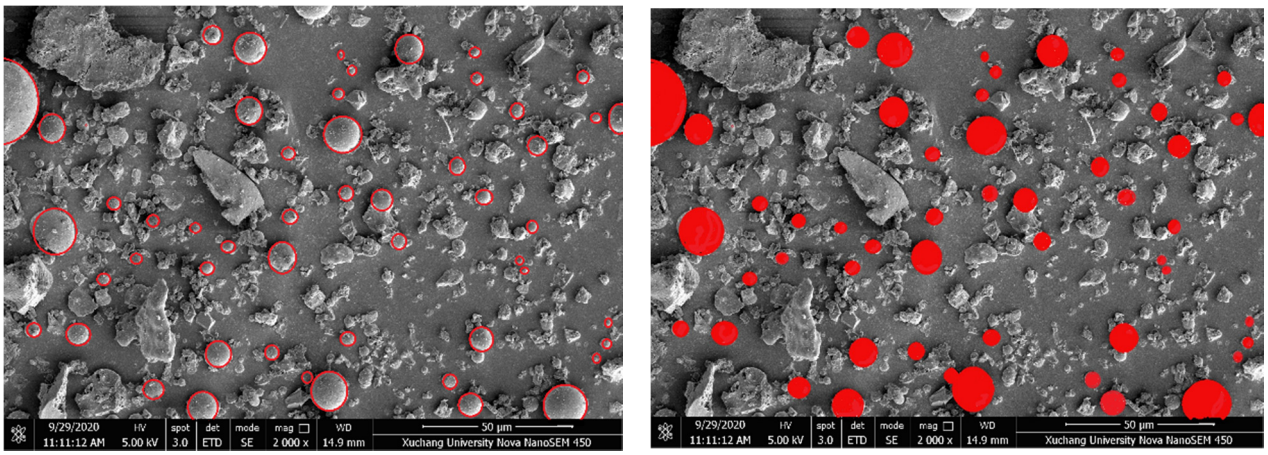

(**a**) Spherical particles (**b**) Coloring of spherical particles

Figure 3. Calculation of spherical particles proportion using SEM-BSE images.

From the spherical particles analysis of different fly ash, the average spherical particles proportion (spherical particles area to all particles area in 50 images) is listed in Table 4.

Table 4. Spherical particles proportion of different fly ash.

Samples	RFA	SFA	GFA
Spherical particles proportion/%	37.64	48.63	17.32

From the calculation of spherical particles proportion, over half of the spherical particles in fly ash was destroyed in the grinding process. Meanwhile, the proportion of spherical particles in SFA was higher than that in RFA. Some studies [30,31] have shown that the particle size of 80% cenospheres in fly ash is below 100 µm. From the particle size distribution curve of SFA, most of the particles were in the range from 5 µm to 150 µm, which led to the higher proportion of spherical particles in SFA.

3.2. Fluidity of Cement Paste Containing Fly Ash

The fluidity analysis results of cement paste containing different fly ash are shown in Figure 4. The fluidity of cement paste could be significantly improved by adding RFA and SFA into fly ash. The fluidity increased with the increasing of fly ash addition from 0% to 40%. However, when ground fly ash was added, the fluidity tended to decrease when the addition was less than 20% and the fluidity was similar when the addition was 0%, 30%, and 40%.

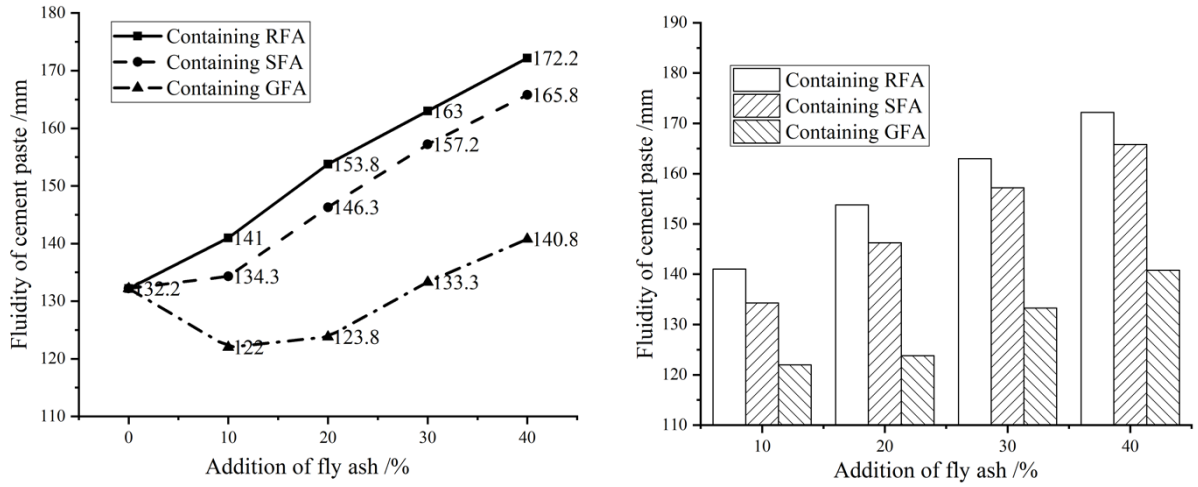

(**a**) Different addition (**b**) Different fly ash

Figure 4. Fluidity of cement paste containing different fly ash.

The results of SEM (Figures 2 and 3) showed that a large number of spherical particles that were identified in RFA and SFA play a ball-bearing effect in the cement paste, which reduces the friction of the interface in the flow process and improves the relative slip between cement particles. From the microscopic morphology of GFA, the proportion of spherical particles was greatly reduced, which weakens the ball-bearing effect and significantly reduces the fluidity of the cement paste containing GFA.

3.3. Shear Rate and Apparent Viscosity of Cement Paste Containing Fly Ash

The rheological properties of cement paste are determined by the yield stress and plastic viscosity of the mixture. In this experiment, the rheological properties of cement paste containing three different kinds of fly ash at different shear rates were analyzed. The shear rate was set to be 0–200 s^{-1} in the experiment and 20 points were taken for analysis. The shear stress and plastic viscosity curves with shear rate change at different additions are shown in Figures 5 and 6.

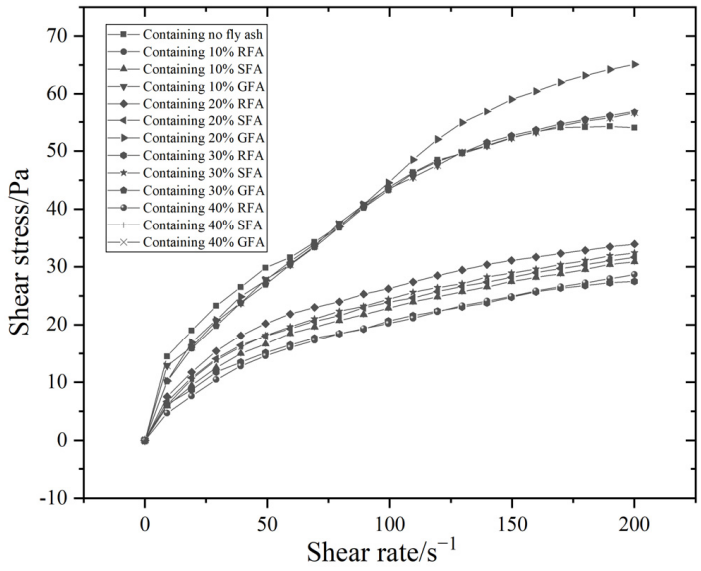

Figure 5. Shear stress of cement paste.

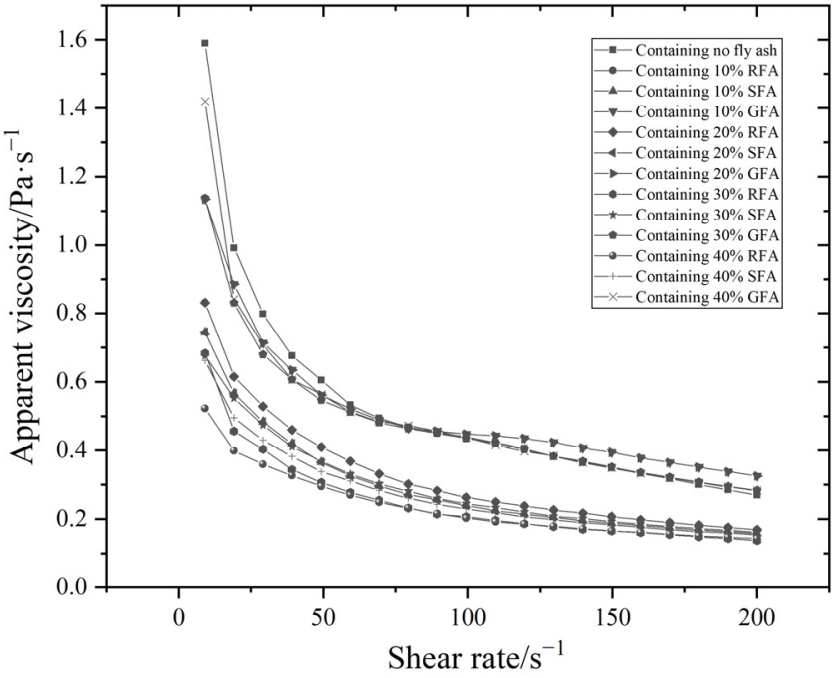

Figure 6. Apparent viscosity of cement paste.

According to the results of shear stress and apparent viscosity, as the shear rate increased, all cement paste samples showed obvious shear thinning phenomenon under shear action, which indicates that the network flocculation structure of cement and fly ash particles in the cement paste was gradually destroyed under shear action, and the apparent viscosity decreased significantly. For samples with different additions of fly ash, cement paste containing no fly ash showed higher shear stress and apparent viscosity which were significantly reduced after RFA and SFA were added, while the evolution laws between samples containing no fly ash and GFA were similar. Many studies [24–26] indicated that the spherical shape of fly ash particles permit greater workability of cement paste as a result of that the ball-bearing effect of fly ash particles reducing the interface friction. A large number of spherical particles in RFA and SFA contributed to the relative sliding between the particles, thereby reducing the shear stress and apparent viscosity of the cement paste. Combining the results of spherical proportion and fluidity test, the rheological properties of fly ash cement paste were closely related to the content of spherical particles.

3.4. Rheological Parameter Analysis of Cement Paste Containing Fly Ash

In order to obtain a better understanding about the influence of different fly ash on the rheological properties of cement paste, the Bingham rheological equation was used to fit the rheological properties of different cement paste and the corresponding yield stress and plastic viscosity were obtained. The rheological equation is shown in Formula (1).

$$\tau = \tau_0 + \eta\gamma \quad (1)$$

where, τ is shear stress, τ_0 is yield stress, η is plastic viscosity, γ is shear rate.

The yield stress and plastic viscosity was calculated and shown in Table 5 and Figure 7.

The rheological parameters calculation results of different samples showed that the yield stress gradually decreased with the increase in RFA and SFA in cement paste, while there was no obvious decrease when GFA was added. From the comparison of different samples, the plastic viscosity of cement paste containing different addition of RFA and SFA was basically the same, which is less than that of cement paste containing no fly ash, and the plastic viscosity showed a certain increasing trend when GFA was added.

Table 5. Rheological parameters of cement paste containing different fly ash.

Sample	Addition of Fly Ash/%	Yield Stress/Pa	Plastic Viscosity/Pa.s	Correlative Coefficient (R^2)
Containing no fly ash	0	15.4946	0.2352	0.8930
Containing RFA	10	9.7184	0.1643	0.9089
	20	9.1302	0.1275	0.8853
	30	8.9291	0.1336	0.8895
	40	8.0769	0.1289	0.9029
Containing SFA	10	9.4274	0.1441	0.8963
	20	10.3691	0.1369	0.8674
	30	7.4696	0.1147	0.9050
	40	6.4368	0.1234	0.9264
Containing GFA	10	13.3846	0.2217	0.8736
	20	11.0847	0.3066	0.9586
	30	12.4537	0.2601	0.9234
	40	13.2997	0.2529	0.9204

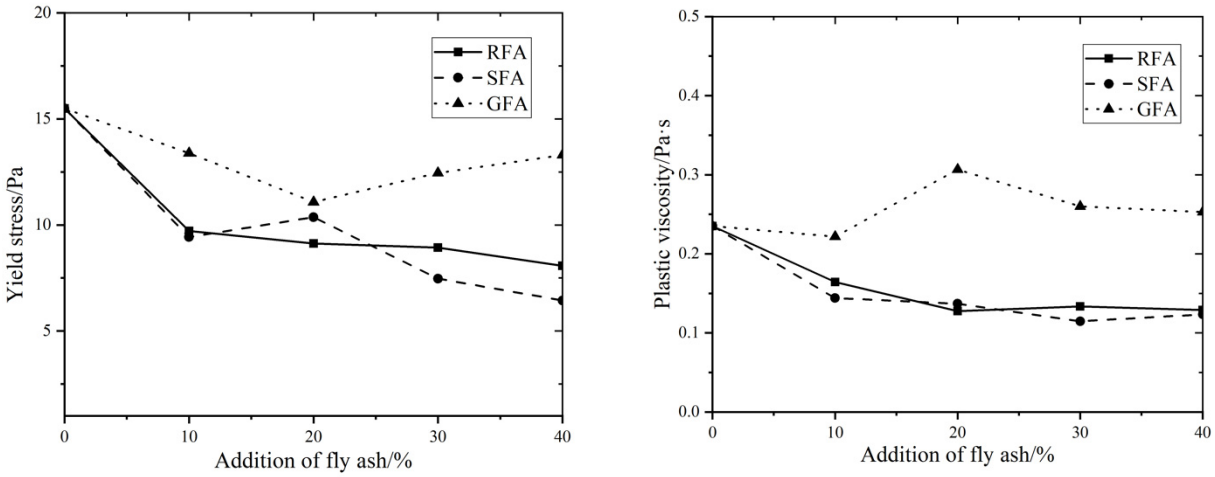

(**a**) Yield stress (**b**) Plastic viscosity

Figure 7. Rheological parameters of cement paste containing different fly ash.

Both RFA and SFA appeared mainly spherical particles while the particle size was different. From the comparison between RFA and SFA in Figure 7, the yield stress and plastic viscosity curves were similar. It indicates that the ball-bearing effect [24] of spherical particles allowed cement paste start to flow under relatively small yield stress, thereby showing smaller yield stress and plastic viscosity.

The particle size range of SFA and GFA was similar while the particle morphology was significantly different. From the comparison between SFA and GFA in Figure 7, the yield stress of cement paste containing GFA was significantly increased. It was equivalent to samples containing no fly ash. Meanwhile, the plastic viscosity was also significantly higher than that of other samples. When the addition of GFA was 20%, the plastic viscosity was the largest. Lanzerstorfer [23] compared the particle shape of the ultrafine fly ash by air classification and by milling, which indicated that milling changes the shape from round to angular while classification does not affect the particle shape. Combined with the observation of particle morphology, a considerable part of spherical particles in the ground fly ash were destroyed and a large number of angular particles were produced, of which the morphology was similar with cement particles. Only if the yield stress was large enough, cement paste was allowed to flow.

3.5. Packing Density of Fly Ash-Cement System

The packing density could reflect the packing state of particles in the cement paste. When the packing density is larger, less water is needed to fill the gaps among the particles which is beneficial to the fluidity of the cement paste. This experiment studied the dry packing states of different fly ash-cement systems. The additions of fly ash in cement paste were 10%, 20%, 30%, and 40%, and the packing density test was tested after mixing uniformly. The results are shown in Figure 8.

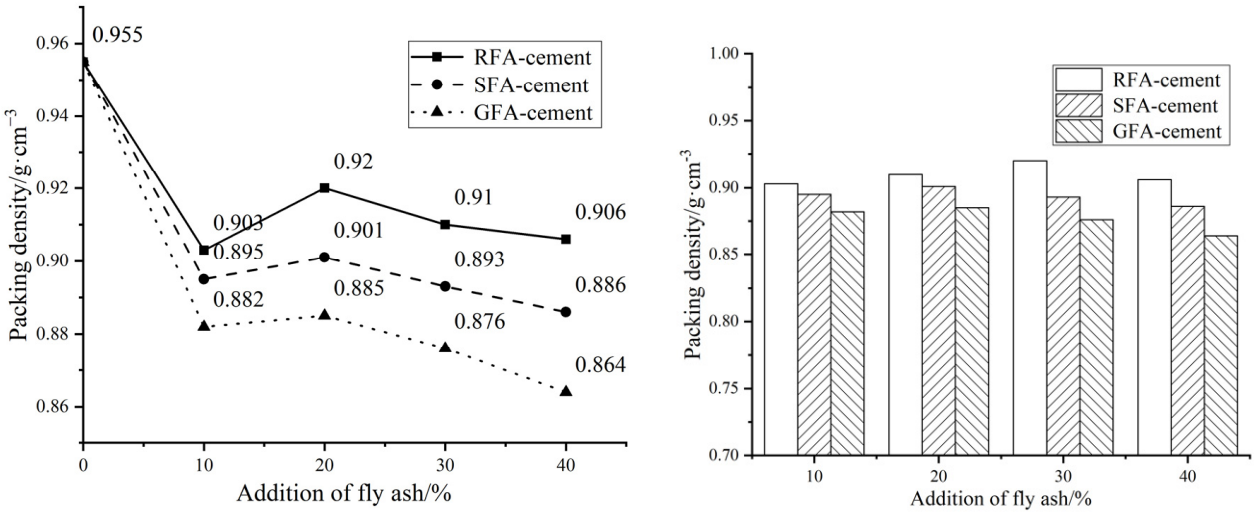

(**a**) Different addition (**b**) Different kind of fly ash

Figure 8. Dry packing density of fly ash-cement system.

According to the dry packing density of different fly ash-cement system, the pure cement system exhibited the highest packing density. It is because the apparent density of cement powder was larger than that of fly ash. The packing density was significantly reduced after adding different kinds of fly ash; however, when the addition reached 20%, each mixed systems showed the highest packing density while the trend decreased again when the addition continued to increase. It indicates that the mixture of 20% fly ash and 80% cement particles showed the relatively densest compact packing structure. According to the rheological parameters of cement paste, cement paste containing 20% fly ash showed the lowest yield stress and the largest plastic viscosity, which is consistent with the packing density results.

From the comparison of different fly ash, RFA-cement system showed higher packing density than SFA-cement system, which indicates that the larger particle size of RFA showed higher packing density after mixing with cement particles. In the cement paste containing SFA of which the particle size was smaller, the agglomeration phenomenon was more likely to appear than in the system of larger particles which leads to a larger porosity particle packing system. In the study of Li [32], the packing density had a clear relationship with the rheological properties of cement paste. Lower packing density and higher specific surface area of powder system indicated a higher water demand and lower workability. In the fly ash-cement mixture ratio, the packing density was lower and more water was required to help flow in the cement paste. Meanwhile, GFA-cement system showed the lowest packing density in all samples, which indicates that the angular particles in the ground fly ash were much easier to form a framework in the packing system, and the packing density decreased with the increasing addition of fly ash, which led to the lowest fluidity of cement paste containing GFA when the water content was the same.

3.6. Zeta Potential Analysis of Cement Paste Containing Fly Ash

The flow state of cement paste is related to the surface charge of the powder particles. The larger the zeta potential value of the powder, the greater the force between the particles, thereby forming a better dispersion effect and improving the fluidity of the cement paste. Cement paste containing different addition of fly ash was prepared and the zeta potential was tested and compared with cement paste containing no fly ash, as shown in Figure 9.

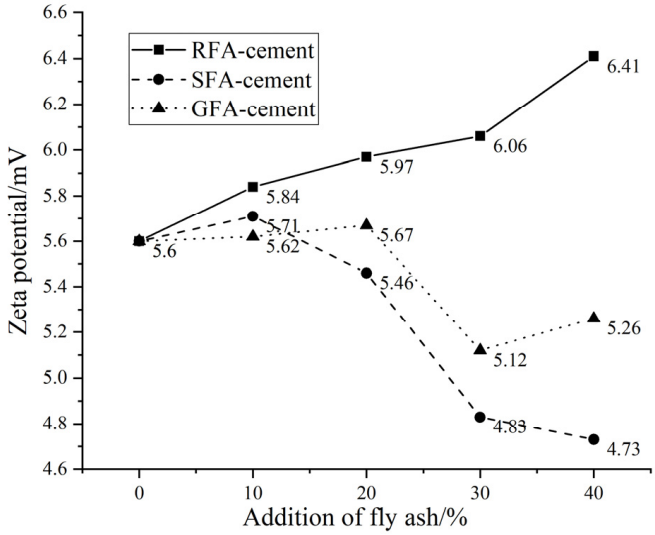

Figure 9. Zeta potential of cement paste containing different fly ash.

From the zeta potential results of different cement pastes, the potential values among the particles of each cement pastes were all positive and the particles exhibited mutually exclusive forces. According to the comparison of different samples, RFA, of which the particle size is relatively largest, showed the largest zeta potential value which increased with the increase in fly ash addition. However, for SFA and GFA, the potential values in the cement paste decreased significantly and it became more obvious when the addition increased. In the studies related with zeta potential and rheological properties of cement paste [33,34], lower zeta potential values caused the tendency of particle agglomeration in cement paste which increased the yield stress. From the comparison of different fly ash, smaller size particles decreased the potential value, which made it more difficult to disperse in the cement paste, thereby the fluidity of cement paste decreased significantly.

4. Conclusions

(1) Compared with the separated fly ash with similar particle size range, some spherical particles of the ground fly ash were destroyed in the grinding process and a large number of angular particles appeared.

(2) The rheological properties of fly ash cement paste were closely related to the content of spherical particles, and the incorporation of ground fly ash below 30% had no positive effect on improving the fluidity of cement paste.

(3) The ground fly ash exhibited a lower packing density and a lower zeta potential value in the fly ash-cement system, which led to the significant increase in the yield stress and plastic viscosity of cement paste containing ground fly ash.

(4) Compared with the separated fly ash, the improvement effect of the ground fly ash obtained by ball mill in laboratory on the working performance of cement paste was relatively weakened. When the addition of ground fly ash exceeded 30%, extra adjustment methods were needed to improve the rheological properties of cement paste.

Author Contributions: Literature search, J.M., H.Z. and D.W.; study design, J.M., H.W. and G.C.; figure, data collection, H.Z.; data analysis, J.M., H.Z. and H.Z.; writing, J.M. and H.Z. All authors have read and agreed to the published version of the manuscript.

Funding: The research has been financially supported by the National Science Foundation of China (No. 51508191), the Science and Technology Project of Henan Province (No. 222102330100), the Foundation from Engineering Research Center of Embankment Safety and Disease Prevention and Control of Ministry of Water Resources (No. DFZX202009), the Master's Innovation ability Enhancement Project of North China University of Water Resources and Electric Power (YK-2021-22).

Institutional Review Board Statement: Not applicable.

Informed Consent Statement: Not applicable.

Data Availability Statement: No applicable.

Acknowledgments: This research has benefited from the experts and laboratory manager of International Joint Research Lab for Eco-building Materials and Engineering of Henan.

Conflicts of Interest: The authors declare no conflict of interest.

References

1. Gullett, B.K.; Linak, W.P.; Touati, A.; Wasson, S.J.; Gatica, S.; King, C.J. Characterization of Air Emissions and Residual Ash from Open Burning of Electronic Wastes during Simulated Rudimentary Recycling Operations. *J. Mater. Cycles Waste Manag.* **2007**, *9*, 69–79. [CrossRef]
2. Palomo, A.; Grutzeck, M.W.; Blanco, M.T. Alkali-Activated Fly Ashes: A Cement for the Future. *Cem. Concr. Res.* **1999**, *29*, 1323–1329. [CrossRef]
3. Yao, Z.T.; Ji, X.S.; Sarker, P.K.; Tang, J.H.; Ge, L.Q.; Xia, M.S.; Xi, Y.Q. A Comprehensive Review on the Applications of Coal Fly Ash. *Earth-Sci. Rev.* **2015**, *141*, 105–121. [CrossRef]
4. Ahmaruzzaman, M. A Review on the Utilization of Fly Ash. *Prog. Energy Combust. Sci.* **2010**, *36*, 327–363. [CrossRef]
5. Krithika, J.; Ramesh Kumar, G.B. Influence of Fly Ash on Concrete—A Systematic Review. *Mater. Today Proc.* **2020**, *33*, 906–911. [CrossRef]
6. Teixeira, E.R.; Camões, A.; Branco, F.G.; Matos, J.C. Effect of Biomass Fly Ash on Fresh and Hardened Properties of High Volume Fly Ash Mortars. *Crystals* **2021**, *11*, 233. [CrossRef]
7. Yadav, V.K.; Yadav, K.K.; Tirth, V.; Jangid, A.; Gnanamoorthy, G.; Choudhary, N.; Islam, S.; Gupta, N.; Son, C.T.; Jeon, B.-H. Recent Advances in Methods for Recovery of Cenospheres from Fly Ash and Their Emerging Applications in Ceramics, Composites, Polymers and Environmental Cleanup. *Crystals* **2021**, *11*, 1067. [CrossRef]
8. Moghaddam, F.; Sirivivatnanon, V.; Vessalas, K. The Effect of Fly Ash Fineness on Heat of Hydration, Microstructure, Flow and Compressive Strength of Blended Cement Pastes. *Case Stud. Constr. Mater.* **2019**, *10*, e00218. [CrossRef]
9. Puthipad, N.; Ouchi, M.; Rath, S.; Attachaiyawuth, A. Enhancement in Self-Compactability and Stability in Volume of Entrained Air in Self-Compacting Concrete with High Volume Fly Ash. *Constr. Build. Mater.* **2016**, *128*, 349–360. [CrossRef]
10. Yu, R.; Spiesz, P.; Brouwers, H.J.H. Development of an Eco-Friendly Ultra-High Performance Concrete (UHPC) with Efficient Cement and Mineral Admixtures Uses. *Cem. Concr. Compos.* **2015**, *55*, 383–394. [CrossRef]
11. Wang, X.; Sun, K.; Li, X.; Ma, J.; Luo, Z. The Effect of Red Mud on Sintering Processes and Minerals of Portland Cement for Roads. *Crystals* **2021**, *11*, 1267. [CrossRef]
12. Zhao, Z.; Wang, K.; Lange, D.A.; Zhou, H.; Wang, W.; Zhu, D. Creep and Thermal Cracking of Ultra-High Volume Fly Ash Mass Concrete at Early Age. *Cem. Concr. Compos.* **2019**, *99*, 191–202. [CrossRef]
13. Mussa, M.H.; Abdulhadi, A.M.; Abbood, I.S.; Mutalib, A.A.; Yaseen, Z.M. Late Age Dynamic Strength of High-Volume Fly Ash Concrete with Nano-Silica and Polypropylene Fibres. *Crystals* **2020**, *10*, 243. [CrossRef]
14. Lam, L.; Wong, Y.L.; Poon, C.S. Degree of Hydration and Gel/Space Ratio of High-Volume Fly Ash/Cement Systems. *Cem. Concr. Res.* **2000**, *30*, 747–756. [CrossRef]
15. Lin, W.-T.; Zhao, W.-Q.; Chang, Y.-H.; Yang, J.-S.; Cheng, A. The Effect of Incorporating Ultra-Fine Spherical Particles on Rheology and Engineering Properties of Commercial Ultra-High-Performance Grout. *Crystals* **2021**, *11*, 1040. [CrossRef]
16. Kara De Maeijer, P.; Craeye, B.; Snellings, R.; Kazemi-Kamyab, H.; Loots, M.; Janssens, K.; Nuyts, G. Effect of Ultra-Fine Fly Ash on Concrete Performance and Durability. *Constr. Build. Mater.* **2020**, *263*, 120493. [CrossRef]
17. Sujay, H.M.; Nair, N.A.; Sudarsana Rao, H.; Sairam, V. Experimental Study on Durability Characteristics of Composite Fiber Reinforced High-Performance Concrete Incorporating Nanosilica and Ultra Fine Fly Ash. *Constr. Build. Mater.* **2020**, *262*, 120738. [CrossRef]
18. Sun, Y.; Wang, K.; Lee, H.S. Prediction of Compressive Strength Development for Blended Cement Mortar Considering Fly Ash Fineness and Replacement Ratio. *Constr. Build. Mater.* **2021**, *271*, 121532. [CrossRef]
19. Gnanaraj, S.C.; Chokkalingam, R.B.; Thankam, G.L.; Pothinathan, S.K.M. Durability Properties of Self-Compacting Concrete Developed with Fly Ash and Ultra Fine Natural Steatite Powder. *J. Mater. Res. Technol.* **2021**, *13*, 431–439. [CrossRef]

20. Krishnaraj, L.; Ravichandran, P.T. Investigation on Grinding Impact of Fly Ash Particles and Its Characterization Analysis in Cement Mortar Composites. *Ain Shams Eng. J.* **2019**, *10*, 267–274. [CrossRef]
21. Zhao, J.; Wang, D.; Wang, X.; Liao, S.; Lin, H. Ultrafine Grinding of Fly Ash with Grinding Aids: Impact on Particle Characteristics of Ultrafine Fly Ash and Properties of Blended Cement Containing Ultrafine Fly Ash. *Constr. Build. Mater.* **2015**, *78*, 250–259. [CrossRef]
22. Fanghui, H.; Qiang, W.; Jingjing, F. The Differences among the Roles of Ground Fly Ash in the Paste, Mortar and Concrete. *Constr. Build. Mater.* **2015**, *93*, 172–179. [CrossRef]
23. Lanzerstorfer, C. Fly Ash from Coal Combustion: Dependence of the Concentration of Various Elements on the Particle Size. *Fuel* **2018**, *228*, 263–271. [CrossRef]
24. Peris Mora, E.; Payá, J.; Monzó, J. Influence of Different Sized Fractions of a Fly Ash on Workability of Mortars. *Cem. Concr. Res.* **1993**, *23*, 917–924. [CrossRef]
25. van der Merwe, E.M.; Prinsloo, L.C.; Mathebula, C.L.; Swart, H.C.; Coetsee, E.; Doucet, F.J. Surface and Bulk Characterization of an Ultrafine South African Coal Fly Ash with Reference to Polymer Applications. *Appl. Surf. Sci.* **2014**, *317*, 73–83. [CrossRef]
26. Rani, R.; Jain, M.K. Effect of Bottom Ash at Different Ratios on Hydraulic Transportation of Fly Ash during Mine Fill. *Powder Technol.* **2017**, *315*, 309–317. [CrossRef]
27. Ferreiro, S.; Herfort, D.; Damtoft, J.S. Effect of Raw Clay Type, Fineness, Water-to-Cement Ratio and Fly Ash Addition on Workability and Strength Performance of Calcined Clay—Limestone Portland Cements. *Cem. Concr. Res.* **2017**, *101*, 1–12. [CrossRef]
28. Ma, J.; Wang, D.; Zhao, S.; Duan, P.; Yang, S. Influence of Particle Morphology of Ground Fly Ash on the Fluidity and Strength of Cement Paste. *Materials* **2021**, *14*, 283. [CrossRef]
29. *GBT 1596-2017*; Fly Ash Used for Cement and Concrete. General Administration of Quality Supervision, Inspection and Quarantine of the People's Republic of China: Beijing, China, 2017.
30. Kolay, P.K.; Bhusal, S. Recovery of Hollow Spherical Particles with Two Different Densities from Coal Fly Ash and Their Characterization. *Fuel* **2014**, *117*, 118–124. [CrossRef]
31. Guo, S.; Ma, C.; Long, G.; Xie, Y. Cleaner One-Part Geopolymer Prepared by Introducing Fly Ash Sinking Spherical Beads: Properties and Geopolymerization Mechanism. *J. Clean. Prod.* **2019**, *219*, 686–697. [CrossRef]
32. Li, D.; Wang, D.; Ren, C.; Rui, Y. Investigation of Rheological Properties of Fresh Cement Paste Containing Ultrafine Circulating Fluidized Bed Fly Ash. *Constr. Build. Mater.* **2018**, *188*, 1007–1013. [CrossRef]
33. Ma, C.; Liu, Y.; Zhou, H.; Jiang, Z.; Ren, W.; He, F. Influencing Mechanism of Mineral Admixtures on Rheological Properties of Fresh Magnesium Phosphate Cement. *Constr. Build. Mater.* **2021**, *288*, 123130. [CrossRef]
34. Sposito, R.; Maier, M.; Beuntner, N.; Thienel, K.-C. Evaluation of Zeta Potential of Calcined Clays and Time-Dependent Flowability of Blended Cements with Customized Polycarboxylate-Based Superplasticizers. *Constr. Build. Mater.* **2021**, *308*, 125061. [CrossRef]